Preparation and Characterization of Polypropylene (PP) Homocomposites: Exploiting Polymorphism of PP Homopolymer

J. Karger-Kocsis[1]*, S. D. Wanjale[2], T. Abraham[2], T. Bárány[1], A. A. Apostolov[3]

[1] Department of Polymer Engineering, Budapest University of Technology and Economics, H-1111 Budapest, Műegyetem rkp. 3, Hungary

[2] Institut für Verbundwerkstoffe GmbH, Technische Universität Kaiserslautern, Erwin-Schrödinger Str., D-67663 Kaiserslautern, Germany.

[3] Laboratory on Structure and Properties of Polymers, Department of Chemistry, Sofia University, J. Bourchier Blvd., BG-1126 Sofia, Bulgaria

* Corresponding Author
E- mail: karger@pt.bme.hu

Abstract

Properties of polypropylene (PP) homocomposites, prepared by film stacking followed by hot pressing were investigated. Alpha- and beta-PP served as matrices, while highly oriented PP tapes of the alpha form acted as reinforcement in the homocomposites. Tapes with different draw ratios (DR=6-12) have been produced and characterized by mechanical and wide-angle X-ray scattering measurements. Tapes with a DR=8 were incorporated in a cross-ply (CP) manner in the corresponding homocomposite laminates. Specimens were subjected to static (tensile, flexural) and dynamic (instrumented falling weight impact (IFWI)) tests. The thermal and thermo-mechanical properties of the PP tapes and homocomposites were studied by differential scanning calorimetry (DSC) and dynamic mechanical thermal analysis (DMTA). The homocomposite morphology was probed by polarized light microscopy that gave evidence of transcrystalline layer at the interface between tape and matrix. The storage modulus of the CP homocomposites was improved prominently by the tape reinforcement. In static tensile tests the homocomposites exhibited much higher stiffness and strength compared to the neat PP specimens. However, this was accompanied with a marked reduction in the ultimate elongation. The IFWI tests showed that both alpha- and the beta-PP failed in macroscopically brittle manner whereas the corresponding homocomposites in semi-ductile way. The homocomposite laminates prepared with beta-PP matrix exhibited higher resistance to penetration than those with alpha-PP.

Key words: composites, impact resistance, polymorphism, structure-property relations, polyolefins

1. Introduction

Polymer homocomposites, containing both reinforcing and matrix phases from the same polymer, became under spot of interest recently. The interest behind this development is mostly due to the low density and easy recycling (via reprocessing) of the corresponding homocomposites. The concept of homocomposites was introduced by Capiati and Porter [1] showing its feasibility on high density polyethylene-based systems. Nowadays, polypropylene (PP)-based homocomposites (also termed self-reinforced or all-PP) are commercially available, such as Pure® and Curv®. Pioneering works for the development of Pure® and Curv® were performed by the groups of Ward [2-5] and Peijs [6-11], respectively. The philosophy of hot compaction, adapted for Curv®, is to transform a part of the reinforcing fiber into the matrix. By contrast, extrusion coating of PP homopolymer tapes by PP copolymers of lower melting temperature is the basic concept of the Pure® production. The properties of both Pure® and Curv® homocomposites have been studied and even compared with those of traditional glass fiber reinforced composites [8-12]. The key issue of the production of polymer homocomposites is to maintain the high stiffness and strength of the reinforcement (usually fibers and tapes with different lay-up or textile architecture), i.e. to avoid their temperature-induced relaxation. To enlarge the processing window, either the melt flowing temperature of the matrix should be reduced, or the melting range of the reinforcement increased, or both. A straightforward method to enhance the melting temperature of the reinforcement is to put it under external load [13] or by using tapes/fibers having very high tenacity (drawing ratio) [14]. Melt temperature reduction from the matrix side can be achieved by using random type PP copolymers, which is a state-of-art approach [15-17]. A further alternative has been proposed by Karger-Kocsis [18], by exploiting the polymorphism of PP. Note that the beta modification of PP melts at markedly lower temperature than the usual alpha modification [19]. Accordingly, PP homocomposites, composed of alpha phase reinforcement and beta phase matrix can be produced [20]. The latter can be achieved by incorporation of selective beta nucleating agents [19,21] in PP homo- and copolymers. It is noteworthy that the polymorphism of other semicrystalline polymers, such as polyamide and polyester, can be exploited to produce the related homocomposites. This was recently shown by the group of Fakirov [22].

In this work, PP homopolymer tapes of different stretching ratio were produced and used as reinforcement. The alpha tapes were embedded in both alpha and beta PP homopolymer having higher melt flowability than the reinforcing PP grade. Homocomposite laminates were manufactured by the film stacking technique using the matrix forming alpha- or beta- PP

homopolymer in the form of films. Properties of the resulting homocomposites were determined under static (tensile, flexural) and dynamic conditions (falling weight impact). Moreover, the thermal and thermo-mechanical properties of the PP tapes and PP homocomposites were also investigated.

2. Experimental

2.1. Materials

For the production of tapes, Moplen® HP400H homopolymer (melt flow index, MFI, at 230°C/2.16 kg = 2 dg/min) of Basell Polyolefins (Rotterdam, The Netherlands) has been selected. As matrix material, Tipplen H388F with nominal MFI value of 8 dg/min of TVK Co. (Tiszújváros, Hungary) served. This H388F grade was processed into film of ca. 0.2 mm thickness in a chill-roll type equipment [23]. The related films consisted of the alpha and beta forms respectively. Beta-PP was achieved by incorporating 0.15 wt% calcium suberate via melt compounding. The beta content of the corresponding film, determined by wide-angle X-ray scattering (WAXS) data using the formula of Turner-Jones et al. [24], was 0.898 [23].

2.2. Tape production and characterization

The PP was first extruded using a twin-screw extruder (Brabender, Duisburg, Germany) having a screw diameter of 25 mm and length to diameter ratio of 22. The temperature in the zones from the hopper to die was 220 and 250°C, respectively, and the screw rotations 10 rpm. The PP tape leaving the rectangular die (7.5x0.48 mm^2) was drawn in a home built stretching unit at 100°C. The home-built stretching line is depicted schematically in Figure 1. Tapes with different draw ratio, viz. 6, 8, 10 and 12, were produced. The draw ratio (DR) was defined by the speed ratio of the final and the initial take-off roller of the stretching unit. The tapes with a draw ratio of 10 exhibited inhomogeneous whereas above this threshold full stress whitening. The resulting tapes (cross section of ca. 1.2x0.1 mm^2) were subjected to differential scanning calorimetry (DSC), wide-angle X-ray scattering (WAXS), dynamic mechanical thermal analysis (DMTA), and static tensile tests.

The melting of the tapes was characterized using a Mettler-Toledo DSC821 instrument (Greifensee, Switzerland). DSC scans were performed from 25°C to 200°C at a heating rate of 10°C/min in nitrogen atmosphere.

The orientation of the tapes was studied by a D500 diffractometer (Siemens, Munich, Germany) using Ni-filtered CuK$_\alpha$ radiation. Two-dimensional (2D) X-ray scans were

collected over 0 to 90° of the azimuthal angle (Φ) for the crystal reflections with Miller indices 110 and 040, respectively.

DMTA (DMTA Q800 TA Instruments, New Castle, USA, equipped with a data acquisition software) tests on the PP tapes (30 mm length, 1.2 mm width and 0.1 mm thickness) were carried out in a tensile mode. The specimens were cooled to -50°C and then temperature sweep was carried out up to 120°C at frequency of 1 Hz and 0.1% strain.

The mechanical properties of these tapes were determined using static tensile tests. A special type of clamping was used for fixing the tapes. This ensured that there was no slippage of the tapes during the tests. The gauge length of the samples was 120 mm and they were deformed by 5 mm/min using a preload of 20 N. The Young's modulus was determined for all specimens at a deformation rate of 1 mm/min using an external extensometer. Eight specimens were tested for each case to ensure the reproducibility.

2.3. Homocomposites preparation and characterization

PP homocomposites were produced by hot pressing of textile laminates of cross-ply (CP) lay-up. In these laminates, the alpha-PP tapes were wound in a CP (0 and 90°) manner in between the matrix-giving beta-PP or alpha-PP films. Further details of this production method are disclosed in our previous paper [20]. Hot consolidation of the above mentioned textile structures was carried out in a Satim hot press (Rion des Landes, France) according to processing cycle given in Figure 2. The homocomposites thus prepared using alpha- and beta-PP were denoted as alpha CP and beta CP respectively. Their nominal reinforcing tape content was 50%.

For the processing temperature (PT) 160°C and 165°C were selected when using the beta- and alpha-PP films, respectively. Note that these temperatures are 10°C and 0°C higher than the DSC melting temperature of the corresponding PP samples.

The morphology of the PP homocomposite was studied on thin sections by polarized light microscopy (PLM) using a microscope of Leitz (Wetzlar, Germany). Thin sections of about 10 μm were cut from the composite by a microtome (Microm, Walldorf, Germany) at room temperature (RT).

DMTA specimens cut from the homopolymer and homocomposite plates had the dimensions: 60 mm (length), 15 mm (width), and 2 mm (thickness). For their DMTA analysis a dual cantilever mode was used. The specimens were cooled to -50°C. The temperature was allowed to stabilize and then increased stepwise, viz. by 3°C, followed by 5 min isothermal

holding, until 120°C. During the DMTA tests at frequency of 1 Hz, the specimens were under 0.1% strain (which was well within the viscoelastic region).

Quasistatic tensile and flexural tests were performed according to the related standards. The deformation rates were 5 and 1 mm/min for tensile and flexural tests respectively, and at least five parallel tests were run at room temperature (RT).

The dynamic impact properties of the homocomposites were determined using instrumented falling weight impact (IFWI) tests. Quadratic specimens (60×60 mm^2) were perforated by a spherical tipped striker of 20 mm diameter. The diameter of the support ring of the specimens was 40 mm. IFWI was performed with incident impact velocity and energy of 4.43 m/s and 229.05 J, respectively on a Dartvis$^{®}$ device of Ceast (Pianezza, Italy). This device was equipped with a DA 16000 data acquisition unit allowing us to monitor/derive the force and energy as functions of both time and displacement.

3. Results and discussion

3.1. PP tapes

The PP tapes with various DR were characterized by DSC. The thermograms indicated that the crystallinity increased from DR-6 to DR-8, but for the tapes of DR-10 and DR-12, it was found to be lower than that of DR-8 (Table 1). The tensile modulus monotonously increased, whereas the strength of the tapes went through a maximum as a function of DR. As described earlier, the tapes with DR-10 exhibited inhomogeneous stress whitening, suggesting the formation of microvoids. The DR-12 tapes were found to be completely stress whitened (due to microvoid formation), as well as partly fibrillated (owing to breakage of the overstressed fibrillar structure). This is the reason why the strength passed a maximum as a function of the DR. By contrast, the modulus of the tape increased monotonously with DR as this response is likely governed by the actual crystalline morphology.

In order to see the orientation dependence on the stretching ratio the azimuthal scans were obtained over 0 to 90° of Φ for the reflexes 110 and 040 of alpha-PP, where Φ is the angle between the chain axis of PP and the stretching direction. These scans are presented in Figure 3 where it is clearly seen that sample DR-12 shows larger distribution of the orientation of the molecules around the stretching direction. For quantitative representation the Hermans' orientation function f was calculated by [25]:

$$f = \frac{3\langle \cos^2 \Phi \rangle - 1}{2} \tag{1}$$

with $\langle \cos^2 \Phi \rangle$ is defined as:

$$\langle \cos^2 \Phi \rangle = \frac{\int_0^{\pi/2} I(\Phi) \cos^2(\Phi) \sin(\Phi) d\Phi}{\int_0^{\pi/2} I(\Phi) \sin(\Phi) d\Phi} \qquad (2)$$

where $I(\Phi)$ is the azimuthal scan intensity. Since there is no suitable plane perpendicular to the chain axis, $\langle \cos^2 2\Phi \rangle$ was calculated from the crystal 110 and 040 reflections according to the proposal of Zuo et al. [26]:

$$\langle \cos^2 \Phi \rangle = 1 - 1.090 \cdot \langle \cos^2 \Phi_{110} \rangle - 0.901 \cdot \langle \cos^2 \Phi_{040} \rangle \qquad (3)$$

The orientation function calculated for the tapes was found to be 0.84 for DR-8 and 0.81 for DR-12. Let us remind that the orientation function equals unity for perfect orientation of the molecules along the stretching direction. The intensity distribution was varied within the standard error. Since the value of f depends only slightly with the intensity distribution, the change of f from 0.84 for sample DR-8 to 0.81 for sample DR-12 should be considered as significant. It seems that for DR > 8 the chain orientation decreases, probably due to void formation and chain breakage.

Table 1 shows the tensile modulus and tensile strength of the tapes with various DR. The tensile modulus increased with increasing draw ratio (the modulus increased from 2.9 GPa at DR-6 to 7.9 GPa for DR-12). The tensile strength of the tapes also increased with the DR up to DR-10 whereas the tape with DR-12 exhibited a slightly lower value than that with DR-10. As argued before, this is due to chain breakage phenomena at high DR. Based on the above findings, tapes with DR-8 were used for the production of composites.

3.2. Polarized light microscopy (PLM)

Microtomed sections served to check the consolidation quality and interphase structure of the laminates. PLM micrograph (Figure 4) taken from the thin microtomed section, suggested that the stretched tape caused alpha transcrystallization in the beta-nucleated PP matrix. This aspect should be checked as a transcrystalline-like layer (termed to cylindrite) appears also when shear deformation takes place at the interface [21, 27]. This is highly probable due to the shrinkage of the tape at the consolidation temperature. Anyway, the formation of this transcrystalline like structure may guarantee an efficient stress transfer from the matrix to the tape reinforcement ([28] and references therein).

3.3. DMTA

The storage modulus (E') and tanδ values as a function of temperature for alpha-PP, beta-PP and PP tape with DR-8 are shown in Figure 5. One can observe that there is no significant difference in the storage moduli of the alpha-PP and beta-PP, while the PP tape with DR-8 exhibited much higher storage modulus (stiffness) compared to the PP matrix materials as expected. This significant increase in the stiffness is attributed to the supermolecular structure and highly oriented polymeric chains in the direction of stretching of the tapes. The tanδ vs. temperature curves signifies different molecular relaxation transitions of the polymer. As can be seen from this figure, the tanδ vs. temperature curves for the PP matrix materials show two relaxation transitions at 0°C and 75°C, respectively. They are assigned to the β and α relaxation transitions, respectively. The relaxation at 0°C corresponds to the glass/rubber transition of the amorphous region (T_g) and the second relaxation transition at 75°C is attributed to the relaxation of polymer chains included in the crystallites and may involve lamellar slippage, too. The tanδ vs. temperature curves are useful to understand the ability of the material to dissipate mechanical energy. Figure 5 indicates that the beta-PP sample exhibited higher tanδ magnitude compared to alpha-PP. This type of behavior was already reported by Karger-Kocsis et al. [29]. The cited authors argued that the higher damping of beta- than alpha-PP represents some toughness improvement. The tanδ vs. temperature curve of the PP tape with DR-8 in Figure 5 displays a different behaviour compared to the matrix materials. The PP tape does not reveal any transition related to T_g in contrast to the matrix-giving PPs. This suggests that the magnitude of chain relaxation in the amorphous region is significantly reduced. On the other hand, the α-transition is well developed at 82°C which is linked to the relaxation of amorphous chains in the crystallites. All these results suggest that the polymer chains and the crystallites are highly oriented along the DR. This shifts the position of the α-transition towards higher temperature and increases its magnitude at the same time.

The dynamic mechanical behavior of the PP homocomposites is shown in Figures 6 and 7. These figures clearly demonstrate the higher stiffness for the homocomposites compared to the neat PPs supporting the reinforcing effect of the PP tapes. The E' at RT (20°C) for the beta-PP and alpha-PP was found to be about 1.8 and 1.9 GPa, respectively, while it increased to 2.7 and 3.8 GPa for the corresponding CP homocomposites. The tanδ values (Figure 7) for

the homocomposites were lower than the matrix-giving PPs. This indicates that the damping of the homocomposites has been substantially reduced due to the PP tape reinforcement.

3.4. Static tensile and flexural tests

Figure 8 shows the typical stress-strain curves for the alpha- and beta-PP-based CP homocomposites. For the sake of comparison this figure also contains the stress-strain response of the alpha- and beta-PP matrix materials. The tensile characteristics are summarized in Table 2. Table 2 and Figure 8 demonstrate that the tensile modulus and yield stress of beta-nucleated PP are lower than those of the alpha-PP. By contrast, the ultimate elongation of beta-PP is much higher than that of alpha-PP. The related change is due to the peculiar lamellar (including tie molecules) and supermolecular structure of beta-PP [21, 30]. As expected, the tape reinforcement strongly enhanced the stiffness and ultimate strength of the homocomposites compared to PP matrix materials. This was accompanied, however, with a marked reduction in the ultimate elongation.

It can be clearly seen in Table 2 that the flexural modulus of alpha- and beta-PP exhibits almost the same values, while the flexural strength of alpha-PP was found to be higher than that of beta-PP. A significant increase in the flexural modulus and strength for the homocomposites, as compared to neat PP matrices, revealed the reinforcing effect of the PP tapes. The flexural strength of the beta-PP CP homocomposite was higher than the alpha-PP version opposed to the stiffness response.

3.5. Instrumented falling weight impact (IFWI) tests

Typical load-time fractograms for the PP matrices and the homocomposites are depicted in Figures 9 and 10, respectively, and the results are summarized in Table 2.

The related fractograms show that both the matrix materials fail in macroscopically brittle manner. Nevertheless, the beta-PP exhibited a markedly higher penetration resistance than the alpha-PP and the energy required for fracture initiation for beta-PP was significantly higher than that for alpha-PP. The fractograms for the alpha-PP shows multiple peaks suggesting the onset of radial cracking. By contrast, the beta-PP matrix specimen failed mostly by circumferential cracking (as demonstrated in Figure 11). For beta-PP a sudden drop in force was observed immediately after the maximum force. These findings agree with the results published in the literature [29].

The benefits of the beta-PP matrix were transferred to the homocomposites containing beta-PP matrices. As can be seen from the Figure 10, the CP homocomposites prepared with beta

nucleated PP exhibited higher perforation energy compared to that for CP homocomposites prepared with alpha-PP matrix. The "noisy" appearance of the fractograms for both the composites after reaching the maximum force is related to the friction of the striker when travelling through the specimen. Both the CP homocomposites were fractured in a similar manner. On the other hand, the homocomposites with beta-PP matrix absorbed more energy than the homocomposite prepared with alpha-PP matrix. The macrophotographs in Fig. 11 indicate that the beta CP was better consolidated than the alpha CP. The better consolidation of beta CP (represented by smaller stress whitened area in the impacted laminates in Fig. 11) compared to the alpha version was observable in the course of the fractograms in Fig. 10 (showing higher forces prior to penetration).

4. Conclusions

Highly oriented alpha-PP tapes (draw ratio, DR=6-12) were produced by on-line drawing an extrudate of rectangular cross section at 100°C. PP homocomposite laminates were prepared using reinforcing tapes of DR=8 which were arranged in a cross-ply manner combining the tape winding and film stacking procedures. The matrices in the homocomposites, consolidated by hot pressing, were the alpha- and beta-forms of PP. Based on this study performed on this novel type of PP homocomposites, the following conclusions can be drawn:

-   with increasing DR of the tapes the tensile modulus monotonously increased whereas the tensile strength passed through a maximum. This was attributed to the development of microvoids affecting only the latter characteristic. The crystal alignment, calculated from 2D WAXS results, likely went through a maximum as a function of DR

-   transcrystalline layer, observed between the tape and the matrix, was made responsible for the stress transfer from the matrix towards the reinforcing tape in the homocomposites

-   static tensile performance of the homocomposite with alpha-PP matrix was superior to that with beta-PP. On the other hand, the homocomposite with beta-PP matrix outperformed the alpha-PP-based one in respect to dynamic perforation impact.

References

1. Capiati, N. J.; Porter, R. S. J Mater Sci 1975, 10, 1671.

2. Abo El-Maaty, M. I.; Bassett, D. C.; Olley, R. H.; Hine, P. J.; Ward, I. M. J Mater Sci 1996, 31, 1157.

3. Ward, I. M.; Hine, P. J. Polymer 2004, 45, 1413.

4. Ward, I. M. Plast Rubber Compos 2005, 33, 189.

5. Hine, P. J.; Ward, I. M.; Jordan N. D.; Olley R.; Bassett, D. C. Polymer 2003, 44, 1117.

6. Peijs, T. Mater Today 2003, 30, 5.

7. Alcock, B.; Cabrera N. O.; Barkoula, N.-M.; Loos, J.; Peijs, T. Compos Part A-Appl S 2006, 37, 716.

8. Alcock, B.; Cabrera N. O.; Barkoula, N.-M.; Loos, J.; Peijs, T. J Appl Polym Sci 2007, 104, 118.

9. Cabrera, N.; Alcock, B.; Klompen, E.; Peijs, T. Appl Compos Mater 2008, 15, 27.

10. Alcock, B.; Cabrera N. O.; Barkoula, N.-M.; Peijs, T. Compos Sci Technol 2006, 66, 1724.

11. Alcock, B.; Cabrera N.O.; Barkoula, N.-M.; Reynolds, C.; Govaert, L.; Peijs, T. Compos Sci Tech 2007, 67 (10), 2061.

12. Abraham, T.; Banik, K.; Karger-Kocsis, J. Express Polym Lett 2007, 1, 519.

13. Barkoula, N.-M.; Peijs, T.; Schimanski, T.; Loos, J. Polym Compos 2005, 26, 114.

14. Izer, A.; Bárány, T. Express Polym Lett 2007, 1, 790.

15. Kitayama, T.; Utsumi, S.; Hamada, H.; Nishino, T.; Kikutani, T.; Ito, H. J Appl Polym Sci 2003, 88, 2875.

16. Houshyar, S.; Shanks, R. A.; Hodzic, A. Macromol Mater Eng 2005, 290, 45.

17. Bárány, T.; Izer, A.; Czigány, T. Plast Rubber Compos 2006, 35, 375.

18. Karger-Kocsis J. Patentschrift DE 10237803B4, Institut für Verbundwerkstoffe GmbH 2007.

19. Varga, J.; Ehrenstein, G.W. Beta-modification of isotactic polypropylene. In "Polypropylene: An A-Z Reference", Karger-Kocsis, J. (ed), Kluwer, Dordrecht, 1999, pp. 51-59.

20. Abraham, T. N.; Siengchin, S.; Karger-Kocsis J. J Mater Sci 2008, 43, 3697.

21. Varga, J. J Macromol Sci - Phys 2002, 41, 1121.

22. Bhattacharyya, D.; Duhovic, M.; Maitrot, P.; Fakirov, S. Express Polym Lett 2009, 3, in press

23. Bárány, T.; Izer A.; Karger-Kocsis J. Polymer Testing 2009, 28, 176.

24. Turner-Jones, A.; Aizlewood, J. M.; Beckett, D. R. Macromol Chem 1964, 75, 134.

25. Wilchinsky, Z. W. J Appl Phys 1960, 31, 1969.

26. Zuo F.; Keum J. K.; Chen, X.; Hsiao, B. S.; Chen, H.; Lai, S.-Y.; Wevers, R.; Li, C. Polymer 2007, 48, 6867.

27. Varga, J.; Karger-Kocsis, J. J Polym Sci Pol Phys 1996, 34, 657.

28. Abraham, T. N.; Wanjale, S. D.; Bárány, T.; Karger-Kocsis, J. Composites A (in press)

29. Karger-Kocsis, J.; Moos, E.; Mudra, I.; Varga, J. J Macromol Sci-Phys 1999, 38, 647.

30. Chen, H. B.; Karger-Kocsis, J.; Wu, J. S.; Varga, J. Polymer 2002, 43, 6505.

Legend of Tables

Table 1

Properties of the PP tapes

Table 2

Static tensile, flexural properties and IFWI perforation energies of the PP matrix materials and PP homocomposites

Designations: E_{peak}: energy absorbed until maximum load (F_{max})

E_{total}: energy absorbed due to full penetration

t: thickness of the specimen

Legend of Figures

Figure 1

Schematic sketch of the hot stretching unit. Note: the speed of the rollers R1,R2 and R3 was the same, while that of R4 varied in order to set the required draw ratio (DR).

Figure 2

Processing cycle for hot pressing of the PP homocomposites.

Figure 3

Azimuthal scans for the PP tapes of DR-8 and DR-12 over the 100 and 040 reflexes. Note: Φ is the angle between the chain axis of PP and the stretching direction.

Figure 4

Polarized light micrograph of the beta CP homocomposite.

Figure 5

Storage modulus (E') and tanδ vs. temperature curves for the alpha- and beta-PP, and PP tape with DR-8.

Figure 6

Storage modulus (E') vs. temperature curves for the PP matrices and corresponding homocomposites.

Figure 7

Storage modulus (E') and tanδ vs. temperature curves for alpha-PP and its homocomposite (alpha CP).

Figure 8

Stress-strain curves for the PP matrices and corresponding CP homocomposites.

Figure 9

Characteristic IFWI fractograms in the form of thickness-related force (F/t) vs. time for alpha- and beta-PP.

Figure 10

Characteristic IFWI fractograms in the form of thickness-related force (F/t) vs. time for the CP homocomposites.

Figure 11

Top views of the failed IFWI specimens of alpha- (a) and beta-PP (b) matrices, and alpha CP (c) and beta CP homocomposites (d). Note: the dimension of the impacted specimens is 60x60 mm^2.

Table 1

| Sample	Width (mm)	Thickness (μm)	Heat of fusion (J/g)	Tensile modulus (GPa)	Tensile strength (MPa)
DR - 6	1.45	150	93.5	2.9±0.1	210±19
DR - 8	1.20	100	101.4	5.3±0.3	266±27
DR - 10	1.10	100	94.9	6.9±0.2	345±20
DR - 12	1.00	90	100.9	7.9±0.2	331±38

Table 2

Specimen	Tensile modulus (GPa)	Yield stress (MPa)	Ultimate elongation (%)	Flexural modulus (GPa)	Flexural strength (MPa)	E_{peak}/t (J/mm)	E_{total}/t (J/mm)
Alpha-PP	1.78	36	17	1.59	53	0.6	0.8
Beta-PP	1.58	28	>100	1.64	45	6.1	6.4
Alpha CP	3.95	94	7	3.08	65	11.6	19.4
Beta CP	2.39	62	8	2.59	72	18.4	26.8
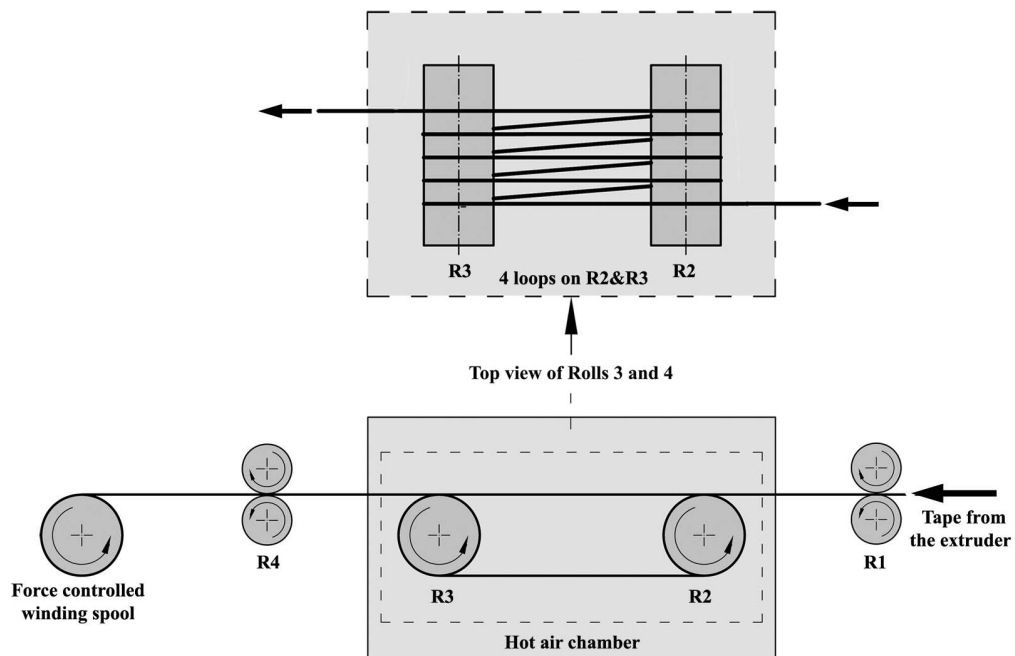
Schematic sketch of the hot stretching unit. Note: the speed of the rollers R1,R2 and R3 was the same, while that of R4 varied in order to set the required draw ratio (DR).
135x89mm (300 x 300 DPI)
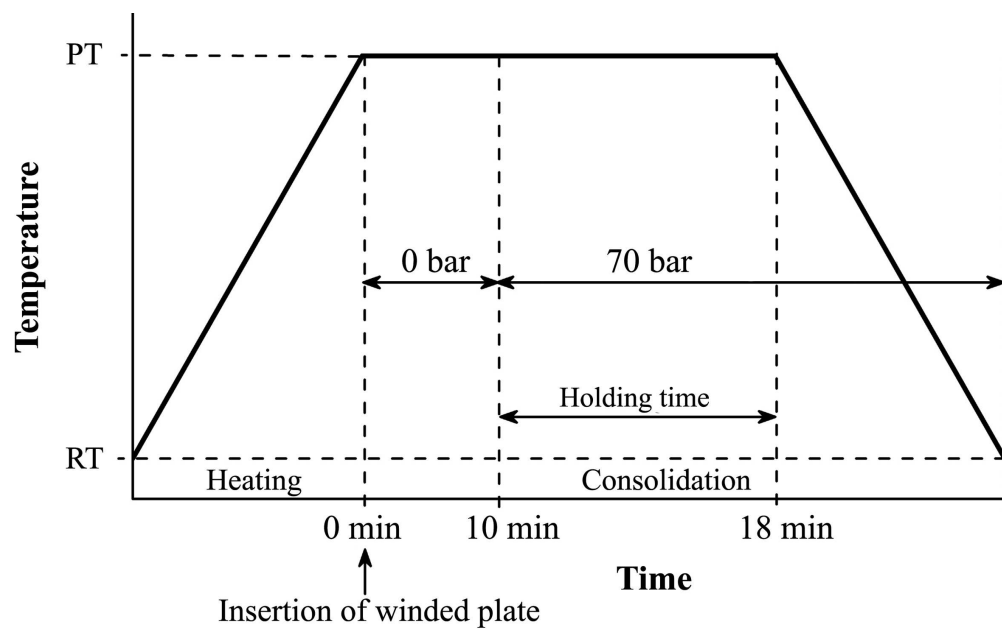
Processing cycle for hot pressing of the PP homocomposites.
99x61mm (599 x 599 DPI)
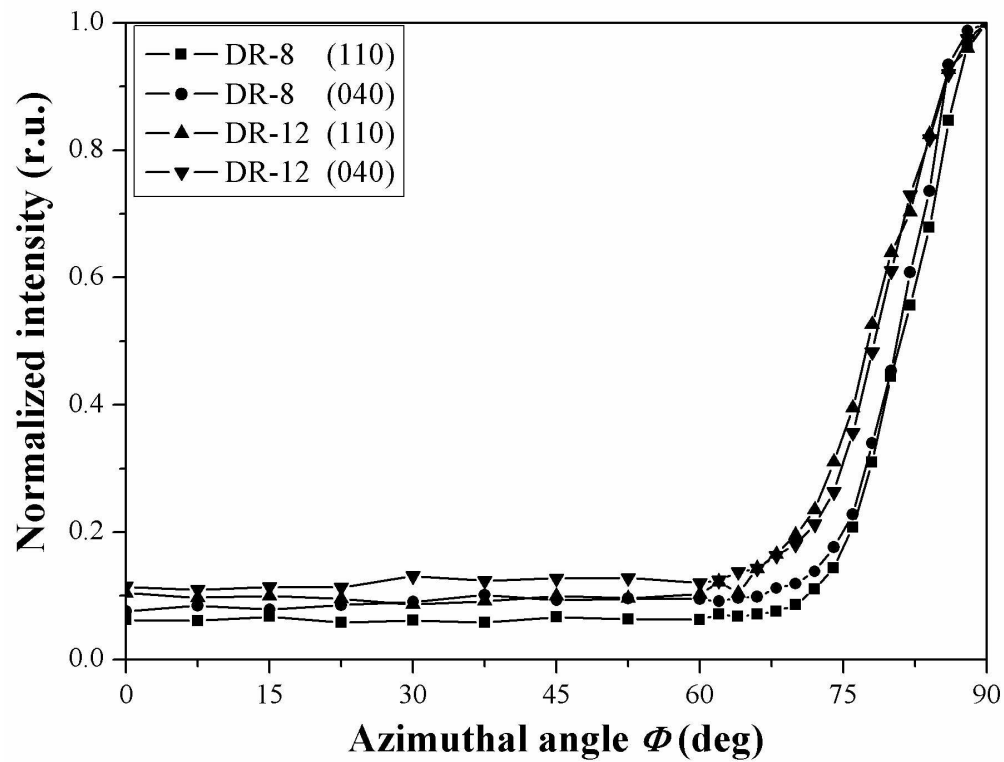
Azimuthal scans for the PP tapes of DR-8 and DR-12 over the 100 and 040 reflexes. Note: Φ is the angle between the chain axis of PP and the stretching direction.
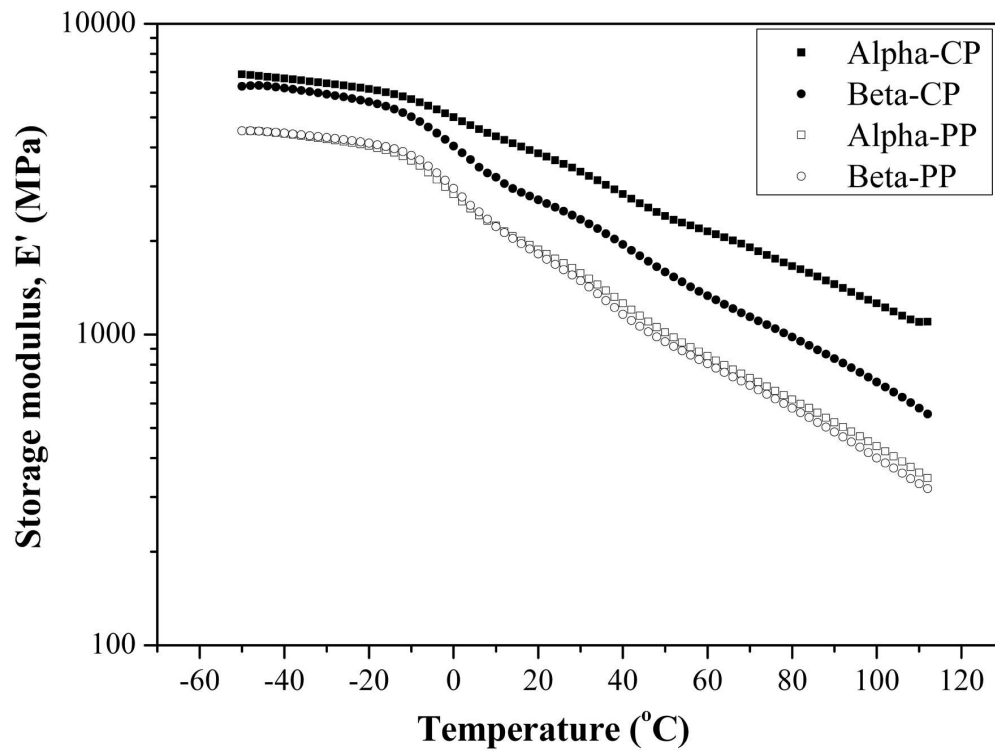152x116mm (300 x 300 DPI)
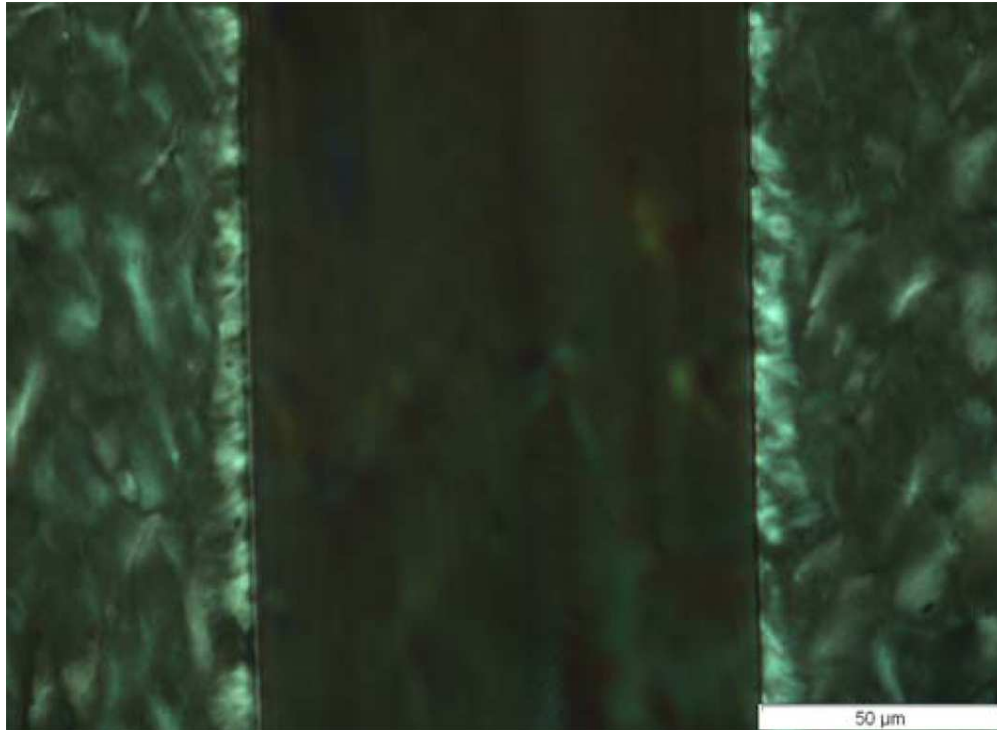
Polarized light micrograph of the beta CP homocomposite.
90x65mm (300 x 300 DPI)
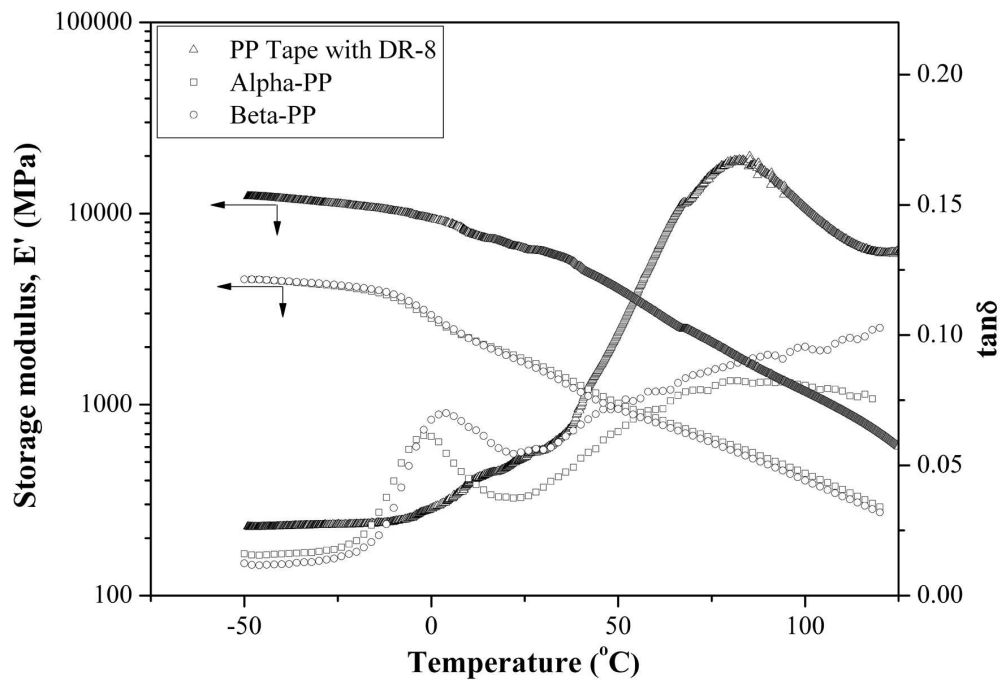
Storage modulus (E') and tanδ vs. temperature curves for the alpha- and beta-PP, and PP tape with DR-8.
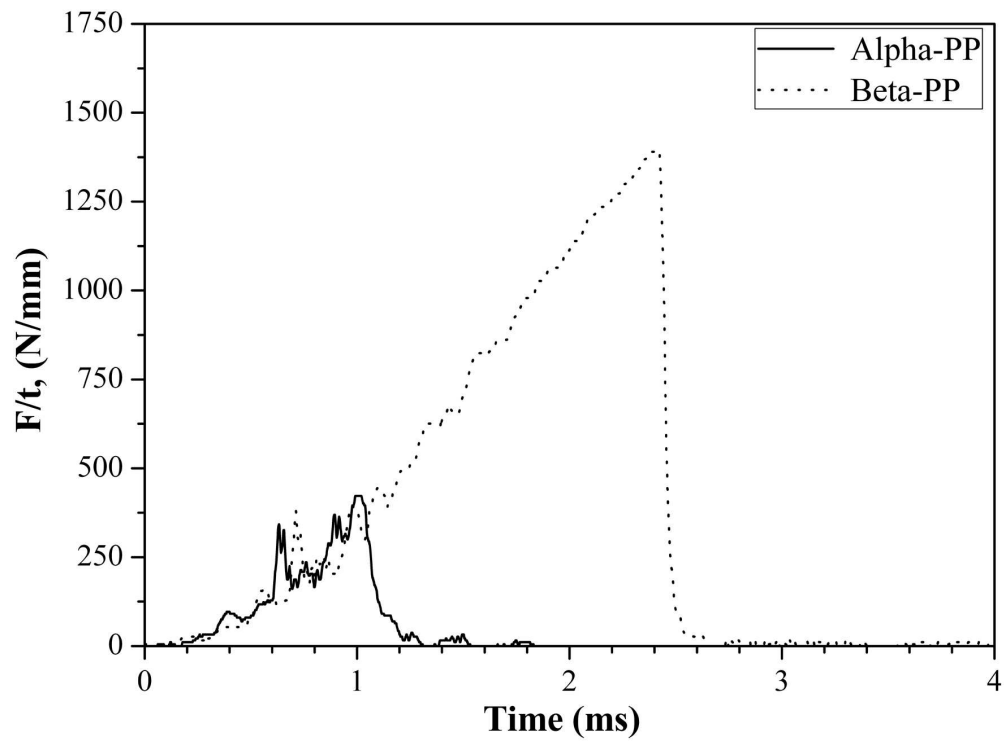150x101mm (300 x 300 DPI)

Storage modulus (E') vs. temperature curves for the PP matrices and corresponding
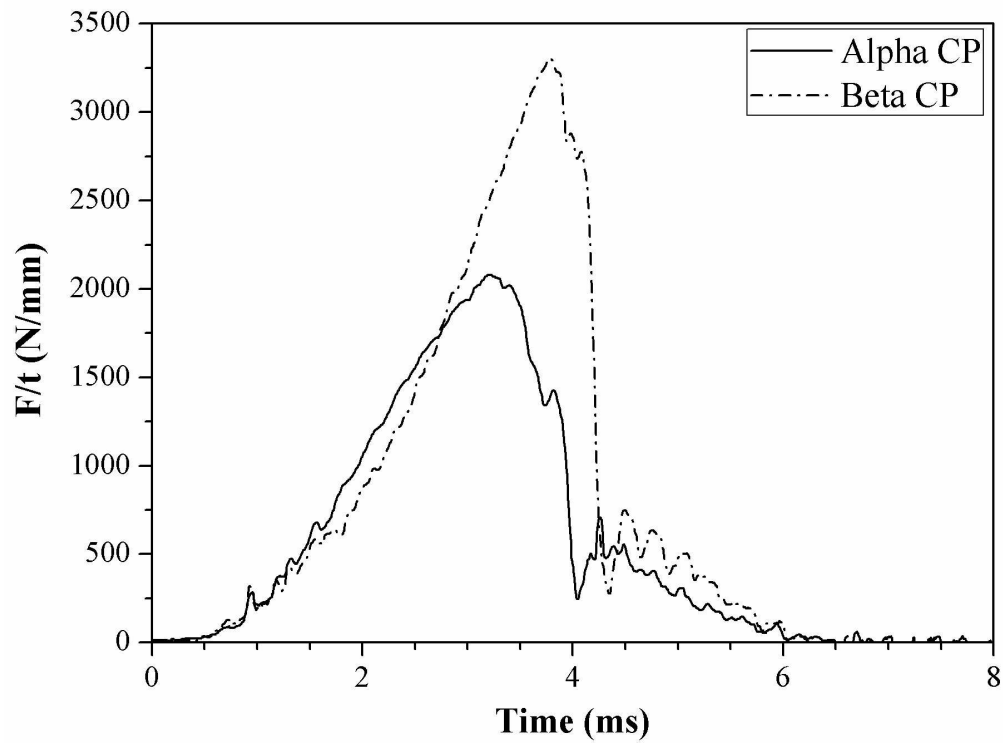homocomposites.
150x112mm (300 x 300 DPI)
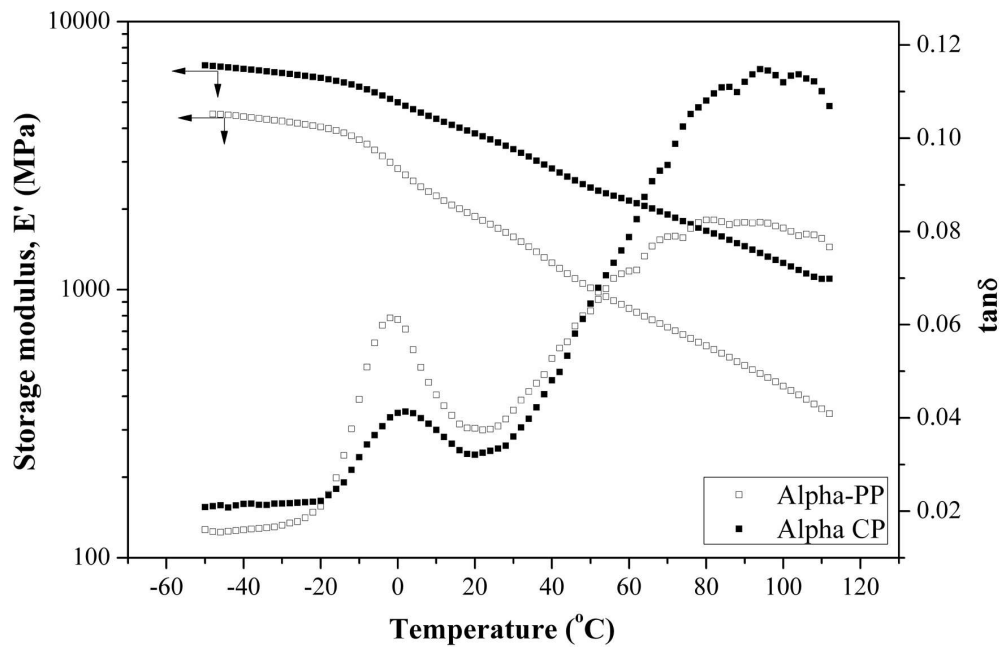
Storage modulus (E') and tanδ vs. temperature curves for alpha-PP and its homocomposite (alpha CP).
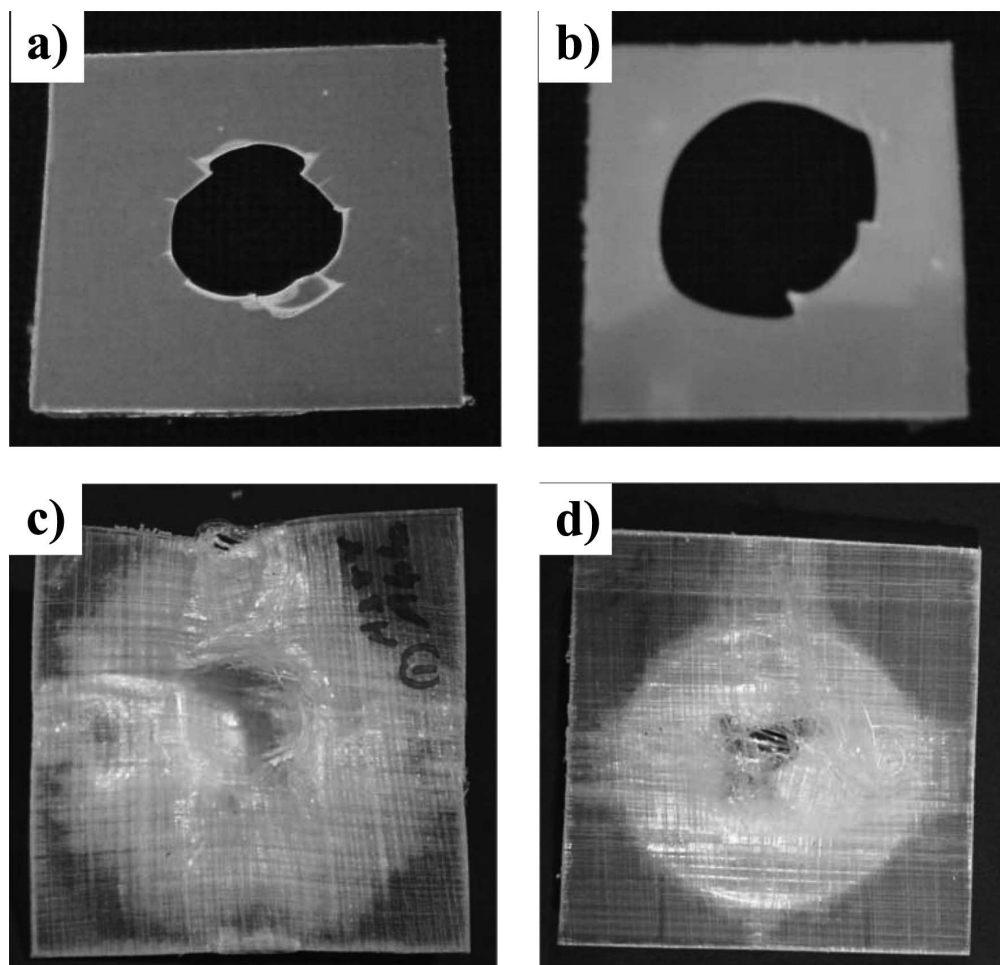150x96mm (300 x 300 DPI)
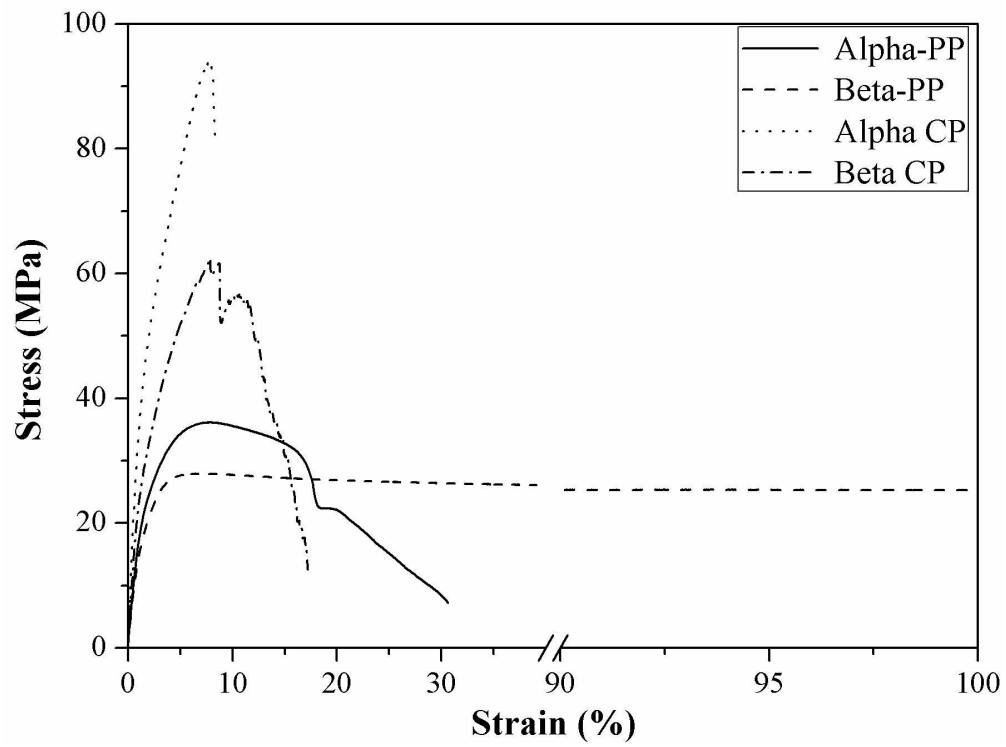
Stress-strain curves for the PP matrices and corresponding CP homocomposites.
152x113mm (300 x 300 DPI)

Characteristic IFWI fractograms in the form of thickness-related force (F/t) vs. time for alpha- and beta-PP.
150x111mm (300 x 300 DPI)

Characteristic IFWI fractograms in the form of thickness-related force (F/t) vs. time for the CP homocomposites.
152x113mm (300 x 300 DPI)

Top views of the failed IFWI specimens of alpha- (a) and beta-PP (b) matrices, and alpha CP (c) and beta CP homocomposites (d). Note: the dimension of the impacted specimens is 60x60 mm². 150x144mm (300 x 300 DPI)